Monte-Carlo simulation of the durability of glass fibre reinforced composite under environmental stress corrosion

N.V. HIEU[a], A. KHENNANE[a], T.TRAN-CONG[a]

[a]Computational Engineering & Science Research Centre (CESRC), Faculty of Engineering and Surveying, University of Southern Queensland - USQ, Australia.

Abstract

The lifetime distribution of glass fibre subject to permanent environmental stress corrosion is very important for assessing the durability and damage tolerance of composites using glass reinforcement. A mechanical model based on the statistics of flaw spectra during stress corrosion and 3D shear lag model is presented. The proposed approach shows that it is possible to identify the influence of stress corrosion properties on the long term durability of glass fibre reinforced composites (GFRP).

Keywords: stress corrosion, shear lag, glass fiber reinforced composite, lifetime durability.

1. Introduction

Fibre-reinforced polymer (FRP) materials are ideal for many engineering applications where high strength-to-weight, stiffness-to-weight ratio, excellent resistances to corrosive substances, and potentially high overall durability are required. Nowadays, composite materials, especially glass fibre composite, are well-suited in applications with greater structural and operational demands, such as low pressure pipes, storage tanks and various structures on offshore drilling platforms. However, the application of composite materials in major civil physical infrastructure has been less enthusiastic, despite the potential economic benefits. The main reason for this is the unknown long-term durability and performance of glass fibre composites. Long-term in this context is 75-100 years. Empirical real-world applications of glass fibre composites rarely extend beyond 40 years and then are seldom well-documented. For glass fibre composites, irrespective of the intended application, long term phenomena need to be accounted for. The three major areas of concern affecting the durability of these materials are

- the fibre-matrix interface
- the matrix
- and, the fibres.

The aging of the matrix and of the fibre-matrix interface is detrimental to the strength of the composite as it impairs the ability to transfer the load among the fibres. Although both are of concern, the main focus of the present study is the durability of the fibres, since these are the critical component of the glass-fibre system. Indeed, the durability of the glass fibres under environment exposure governs many of the fibre-dominated mechanical

properties of glass-fibre structural elements and systems. The strength of glass fibre is a function of the magnitude and duration of permanent loads as well as handling and storage conditions. It is also affected by the environment to which the glass fibres and the fibre-composite are exposed. The main aim of the present investigation is to develop a model based on fracture mechanics, three dimensional shear lag theory, and a probability model for flaw size to study the effect of stress corrosion properties of glass as well as the effect of handling and storage histories of the fibres on the long term durability of the composite. Several numerical simulations were performed using different types of glass in an aqueous environment to estimate the lifetime distribution of the unidirectional composite.

2. Modelling of stress corrosion cracking in glass fibre

Glass fibres contain surface flaws, which usually are the result of atmospheric attack, fibres rubbing together, heat treatment or generated during the drawing. The flaws play a major role in the initiation and propagation of stress-corrosion cracks in the fibres. According to Sekine et al. [1,8], a crack initiates at one of these pre-existing surface flaws and grows perpendicular to the longitudinal axis as shown on Figure 1.

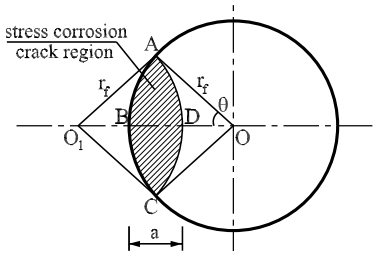

Figure 1: Shape of stress corrosion crack in the fibre.

Following the work by Wiederhorn and Bolz [11], Sekine et al. [1,8], the equation for the stress corrosion rate can be rewritten as

$$\frac{da}{dt} = C \exp\left(\frac{\alpha K_I}{RT} \right), \tag{1}$$

with

$$C = C_w = \upsilon \exp\left(-\frac{E_a}{RT} \right) \quad \text{for aqueous environment.}$$

where a is the length of crack; E_a is the activation energy; K_I is the crack tip stress intensity factor for opening mode I; R is the gas constant; T is the absolute temperature; υ and α are empirical constants.

By approximating the shape of the crack front as a circular arc of radius r_f, Sekine rewrote Eq. (1) in the form of the increasing rate of the half angle θ with time as follows

$$\frac{d\theta}{dt} = \frac{C}{2r \sin\theta} \exp\left(\frac{\alpha K_I}{RT} \right), \tag{2}$$

with the stress intensity factor K_I approximated as

$$K_I = \sigma\sqrt{(1-\cos\theta)2\pi r}\ . \tag{3}$$

Integrating Eq. (2) between initial angle θ_0 and final angle θ_F we find the final time t_F that takes for a fibre to break under stress corrosion as

$$t_F = \frac{4rRT}{C\alpha\sigma\sqrt{\pi r}}\left(\frac{RT}{2\alpha\sigma\sqrt{\pi r}}+\frac{\theta_0}{2}\right)\exp\left(-\frac{\alpha\sigma\sqrt{\pi r}}{RT}\theta_0\right). \tag{4}$$

Equation (4) determines the stress corrosion lifetime of a glass fibre if the parameters υ, α and E are known. These parameters can be determined by experiment and depend on the environment, temperature and glass type.

3. Three dimensional shear lag analysis

In a real unidirectional composite, the stress in an individual fibre depends on the overall applied stress but also on how the stress is transferred from a broken fibre to the surroundings. For a unidirectional composite subject to environmental stress corrosion (ESC), a mathematical description is needed for the redistribution of stresses in broken fibres to the neighboring unbroken ones. The 3-D shear lag model of Okabe et al [6] shown on figure 2 provides a computationally efficient method to achieve this. The model assumes that the fibres are uniformly spaced by a distance *d*. It is composed of *NxM* fibres with an overall length *L*. Each fibre is divided into *K* element. The fibres are treated as one dimensional spring elements that sustain axial force only. The matrix is modelled as an array of shear springs coupling the fibre nodes and its behaviour is controlled only by the axial displacements of the nodes bounding the matrix region. According to the shear lag assumption, there is no normal stress inside the matrix, the equilibrium equation for the stress $\sigma_{i,j,k}$ on the single fibre element is given by

$$A_f\frac{d\sigma_{i,j,k}}{dz} = -\frac{\pi r}{2}\sum_{l=1}^{4}\tau_{i,j,k}^{(l)}\ , \tag{5}$$

where A_f is the area of fiber cross section, the subscript *(i,j,k)* denotes the *(i,j,k)*th node or fibre element, *r* is the fibre radius and $\tau_{i,j,k}^{(l)}$ is the interfacial shear stress in the matrix bounding the considered fibre with *l* ranging from 1 to 4 as shown on figure 2. If there is no matrix yielding, interface yielding, or matrix debonding, the shear stress $\tau_{i,j,k}^{(l)}$ in the matrix can be determined as follows

$$\begin{aligned}
&\tau_{i,j,k}^{(1)} = G_m\frac{u_{i+1,j,k}-u_{i,j,k}}{d};\quad \tau_{i,j,k}^{(2)} = G_m\frac{u_{i,j+1,k}-u_{i,j,k}}{d},\\
&\tau_{i,j,k}^{(3)} = G_m\frac{u_{i\text{-}1,j,k}-u_{i,j,k}}{d};\quad \tau_{i,j,k}^{(4)} = G_m\frac{u_{i,j-1,k}-u_{i,j,k}}{d}.
\end{aligned} \tag{6}$$

where G_m is the matrix shear modulus, $u_{i,j,k}$ refers to nodal displacement at the *(i,j,k)*$^{\text{th}}$ node.

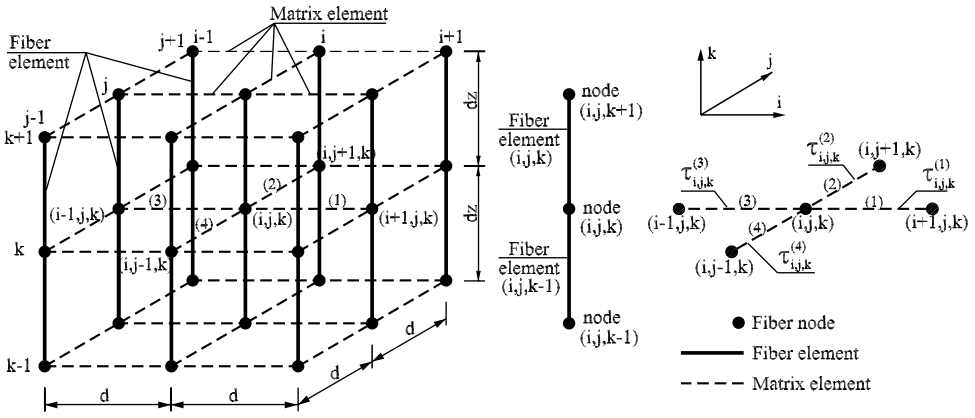

Figure 2: 3D shear lag modelling.

The stress-strain relation in the constituents of this study are shown on figure 3. A fiber element is assumed to be linear elastic with tensile strength σ_e. The matrix behavior is approximated as elastic-perfectly-plastic with shear yielding stress τ_y. The condition for interfacial debonding are not well-established since experimental verification is not easy.

a) b)

Figure 3: The stress-strain relation: a) Fiber; b) Matrix.

The finite difference scheme for solving Eq (5) according to [5,6] is proposed as

$$\frac{4E_f A_f\left[\gamma_{i,j,k}(u_{i,j,k+1}-u_{i,j,k})-\gamma_{i,j,k-1}(u_{i,j,k}-u_{i,j,k-1})\right]}{\left(2+\gamma_{i,j,k-1}+\gamma_{i,j,k}\right)dz^2}+\frac{\pi r}{2}\sum_{l=1}^{4}\left[\tau_{i,j,k}^{(l)}\left(1-P_{i,j,k}^{(l)}\right)+\zeta_{i,j,k}^{(l)}P_{i,j,k}^{(l)}\tau_y\right]=0, \qquad (7)$$

with $\gamma_{i,j,k}=\begin{cases}0\rightarrow \text{element between } (i,j,k) \text{ and } (i,j,k+1) \text{ is broken,}\\ 1\rightarrow \text{element between } (i,j,k) \text{ and } (i,j,k+1) \text{ is not broken,}\end{cases}$

$$P_{i,j,k}^{(l)}=\begin{cases}0, & \text{if } \left|\tau_{\mathrm{i,j,k}}^{(l)}\right|\le\tau_y,\\ 1, & \text{if } \left|\tau_{\mathrm{i,j,k}}^{(l)}\right|\ge\tau_y,\end{cases}$$

where the parameter $\zeta_{i,j,k}^{(l)}$, which determine the sliding direction, is 1 or -1 depending on the sign of the difference in relative displacement between adjacent elements.

Under uniaxial tensile loading, we apply the geometrical boundary conditions

$$u_{i,j,1}=0 \text{ and } u_{i,j,K+1}=\varepsilon_c L. \qquad (8)$$

where ε_c is the applied composite strain; $i=1...N$; $j=1...M$ and L is the fibre length

The axial fibre stress for a fibre element is calculated using the converged nodal displacement from Eq. (7) as

$$\sigma_{i,j,k} = E_f \left(\frac{u_{i,j,k+1} - u_{i,j,k}}{dz} \right). \tag{9}$$

The average applied stress exerted at the end of the specimen (k=K) is given by

$$\begin{aligned} \sigma_{app} &= V_f \sigma_b + (1 - V_f)\sigma_m , \\ \text{with } \sigma_b &= \left(\frac{1}{N \times M} \sum_{i=1}^{N} \sum_{j=1}^{M} \sigma_{i,j,K} \right). \end{aligned} \tag{10}$$

where σ_b and σ_m are fiber bundle and matrix stresses, respectively. We assume that σ_m=0 as the load subjected by the matrix in glass fiber composite is very small in compared with σ_b.

4. Numerical implementation

4.1. Determination of the flaw spectrum

Equation (4) defining the life of a fibre element of length dz subject to stress corrosion suggests that the fibre contains an initial flaw of size θ_o. If it is to be implemented within the framework of the shear lag model defined above, the spectrum of the initial flaws in the fibre elements must be defined. To define the initial flaw spectrum in the fibre elements, fibre strength at different gauge lengths will be used since it is the most easily measured characteristic. It can be interpreted as a measure of the severity of the flaw, and therefore an indication of its depth. Based on the Poisson-Weibull statistics for fibre strengths [10], the strength of every fibre element is independent and the distribution function for the strength can be well approximated by the two-parameter Weibull distribution. Each discretized fibre element of length L loaded to a tensile stress σ has a probability of failure $F(\sigma)$, defined as

$$F(\sigma) = 1 - \exp\left(-\frac{L}{L_o} \left(\frac{\sigma}{\sigma_o} \right)^{\rho} \right), \tag{11}$$

where σ_o and ρ are Weibull scale and shape parameters, respectively. L_o is the original gage length at which the single filament tension tests were performed and the Weibull parameters estimated. L is the extrapolated length of interest (L=dz in this study).

To reproduce a unidirectional composite consisting of fibers obeying the Weibull distribution, we choose a random number η taken from the uniform distribution on the interval [0,1] and allocate the following strength ($\sigma_{i,j,k}$) to each fiber element as

$$\sigma_{i,j,k} = \sigma_o \left[\frac{L_o}{dz} \ln\left(\frac{1}{1-\eta} \right) \right]^{\frac{1}{\rho}}. \tag{12}$$

Following Eq. (3) when the stress is sufficient to cause the maximum value of the stress intesity factor K_I to reach the fiber toughness K_{IC}, we can caculated the half angle flaw of each fiber element $\theta_{i,j,k}$ for assigning with Weibull distribution as

$$\theta_{i,j,k} = \cos^{-1}\left(1 - \frac{K_{IC}^2}{2\pi r \sigma_{i,j,k}^2}\right). \tag{13}$$

4.2. Monte-Carlo simulation

The present simulation for the time-to-failure of GFRP composite under aqueous environment following a scheme similar to that deveploed by Khennane and Melchers [3] is shown on figure 4.

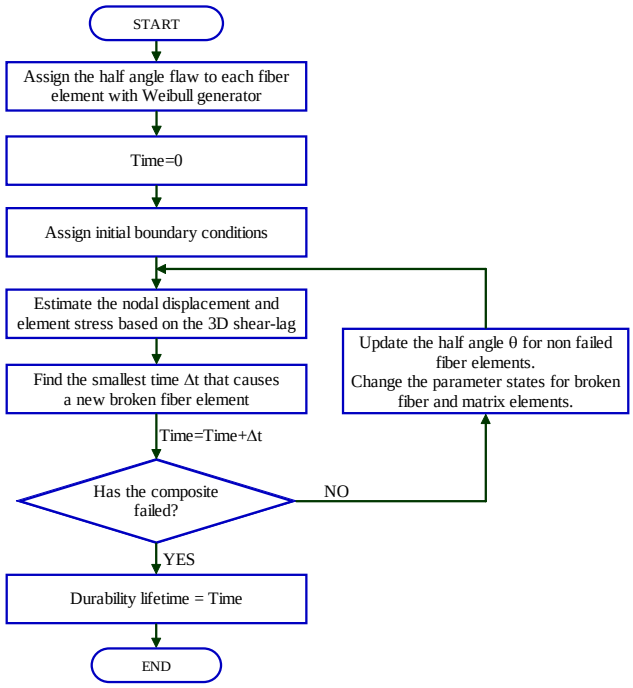

Figure 4: Flow chart of the Monte Carlo simulation.

5. Results and discussion

5.1. Verification of simulated program

The numerical simulations of the time-to-failure under environmental stress corrosion for GFRP were conducted following the described simulation procedure. The stress corrosion data of glass in water [11] is shown in table 1. The mechanical properties of the materials used for the simulations are shown in the table 2. It should be noted that the simulated lifetime would change with different runs. It also depends on the number of fibers (M×N) and the longitudinal segment size (dz) of the model. In order to assess the

effect of these parameters, several different models have been analysed. Owing to computation time constraints, 20 simulations were run for each of models. For N×M=10×10, the variation of the simulated lifetime with the number of longitudinal segments is shown on figure 5.

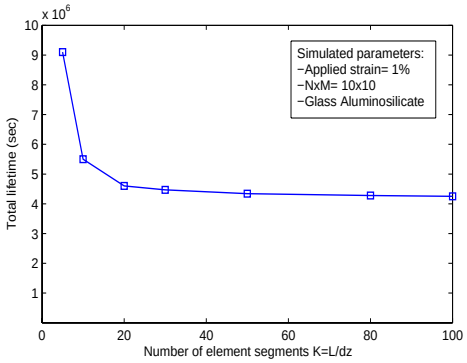

Figure 5: The relation between lifetime and the number of longitudinal segments.

It can be seen on figure 5 that the simulated results approach almost a stationary value when K=50 or more. Thus in the following numerical simulations, K will be taken as 50 to minimize discretization errors. In addition, reasonable numbers of fibres (M×N) should be chosen according to the required accuracy of the results and the acceptable time of simulation. Following the investigation of Okabe et al. [7], who suggested that the number of fibres should be taken as 100 or more, models with M×N=15×15=225 fibres were used in the present simulations. In this study, we do not discuss the size scaling effect on lifetime failure process of composite. These issues are still under further investigations.

Table 1. Stress corrosion data of glass in water [11]

Glass	E_a (J/mol)	α ($m^{5/2}$/mol)	Ln(υ_o)
Aluminosilicate	1.212E5	0.138±0.003	5.5±0.4
Lead-alkali	1.056E5	0.144±0.006	6.7±0.6
Soda-lime	1.088E5	0.110±0.004	10.3±0.5

Table 2. Material properties [6]

Fibre Young's modulus E_f	76000 Mpa
Fibre radius r_f	6.5μm
Fibre volume fraction V_f	0.542
Fibre Weibull shape parameter ρ	6.34
Fibre gage length L_o	24 mm
Fibre strength σ_o based on gage length L_o	1550 MPa
Fibre fracture toughness K_{IC}	0.77 MPa
Matrix Young's modulus E_m	3400 MPa
Matrix yield shear stress τ_y	42 MPa
Matrix poisson's ratio ν	0.35

Due to the lack of experimental data, the obtained results are compared to a similar finite element analysis developed by Khennane and Melchers [4] as shown on figure 6. It can be seen that this present analysis showed good agreement with the finite element

method (the difference is lower than 2%), thus verifying the present model. Nonetheless, the model still requires further validation with experimental data.

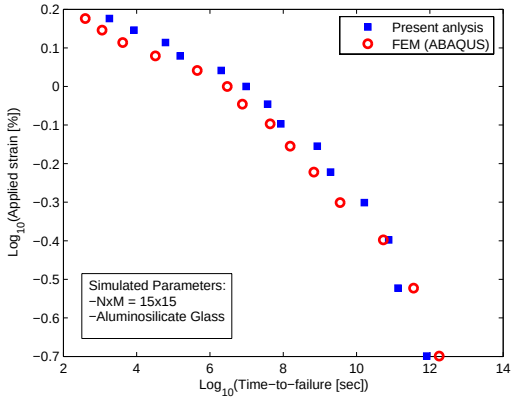

Figure 6: Comparison the present analysis with FEM ([4]).

Figure 7a. shows the accumulation with time of fibre breaks for an Aluminosilicate glass composite under different applied strain levels. It can be seen that an incubation period is present in all the results, and is shorter at higher applied strains.

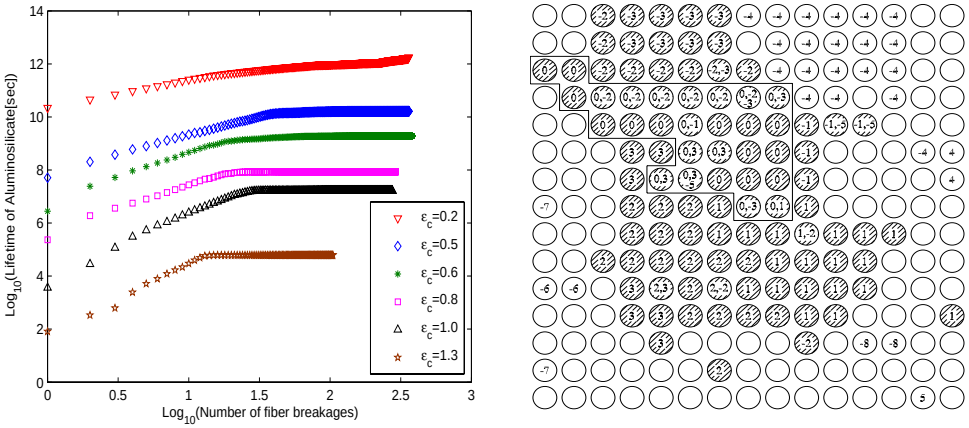

a) at different applied strains b) cross-section of critical plane

Figure 7: Fibre break distribution of Aluminosilicate glass.

Figure 7b represents the distribution of breaks in the Aluminosilicate composite just prior to failure. The charts in figure 7b is a schematic representation of the cross-section in the failure plane. Each number in a circle represents a break along that fibre. A zero represents the final failure plane, 1 is a break on the plane above the failure plane, -1 is one plane below and so forth. Breaks that are most likely linking up to produce the final separation of the composite are hatched. It can be seen that the damage evolution has a very large cluster of breaks in the plane that drives the continued growth of cracks leading to the clear-cut final failure plane. This is consistent with the Local Load Sharing (LLS) concept.

5.2 Numerical lifetime simulations

For examination of the effect of aqueous environment on the glass type, simulations were carried out for three type of glass fibres as shown on table 1. The results of lifetime distribution at different applied strain are shown on figure 8.

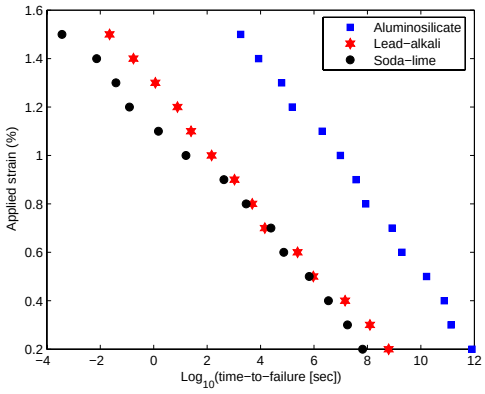

Figure 8: Lifetime distribution of glass fibres in aqueous environment.

As can be seen, the type of glass has a considerable influence on the stress corrosion of a glass fibre. The glasses with high content of Na_2O, which is known to be the major contribution to stress corrosion [2], show the shortest lifetime. From figure 8, it can be seen that the Aluminosilicate glass (containing the lowest Na_2O) has the highest lifetime distribution under stress corrosion while the Soda-lime glass (containing the highest Na_2O) exhibits the shortest lifetime.

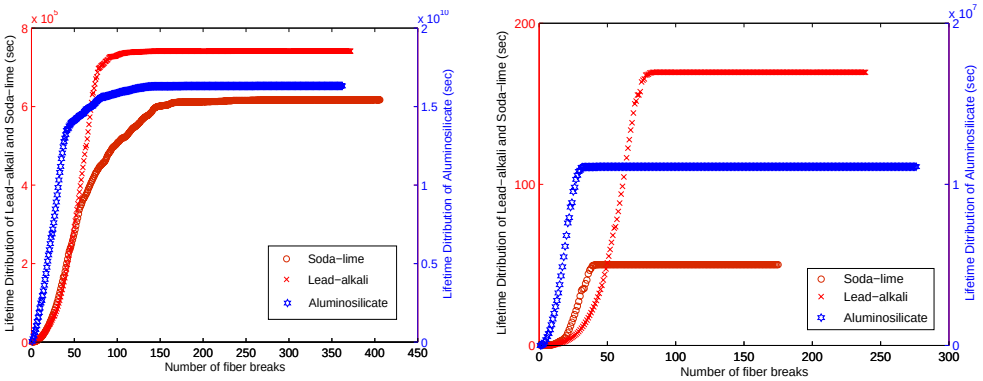

a) at the applied strain 0.5% b) at the applied strain 1%

Figure 9: Fibre break distribution at low and high applied strain.

Figure 9a shows the incubation of fibre breaks for three kinds of glasses under low applied strain 0.5%. When comparing these plots, it can be noticed that about one third of fibres fail sequentially, and this lasts for about 99% of the life of the composite. Then the composite fails suddenly in a brief succession of fibre breaks. This is consistent with experimental observations reported by Swit (2000) [9]. As the level of applied strain

increase to 1% (figure 9b), the incubation period covers less than a third of fibre breaks (about 1/10 for Alumino-silicate, about 1/5 for Soda-lime and Lead-alkali) and failure of the composite is more sudden.

6. Conclusion

This paper presented a simulation of the lifetime distribution of GFRP composite based on the chemical behaviour of glass, 3D shear lag method and Monte-Carlo technique. These were combined with fracture mechanics, the finite difference method and a probability model for flaw size to develop a model for the description of the behaviour of GFRP composite subject to stress corrosion in three dimensions. The stress corrosion of glass fibres was found to depend on the type of glass and environmental conditions. Stress corrosion cracking of GFRP was also found to have an incubation period before the stress concentration reaches such a high level that unstable crack growth occurs. This behaviour is consistent with the generally recognized catastrophic failure of composites under static fatigue [9]. Finally, the results of the present study, although limited to rather idealized situations, are very encouraging. They suggest that, with only modest assumptions about material properties, it is possible to obtain model mechanisms of GFRP breakdown and to permit an estimation of the time-to-failure under environmental stress corrosion.

7. References

[1]. Beaumont PW.R, Sekine H. Physical modelling of engineering problems of composites and structures. *Applied Composite Materials* 2000 ; **07:** 13-37.

[2]. Charles R.J. Static fatigue of glass. *Journal of Applied Physics* 1958, **29:** 1549-1560

[3]. Khennane A, Melchers R. E. Durability of glass polymer composites subject to stress corrosion. *ASCE Journal of Composite for Construction* 2003 ; **07:** 10-117.

[4]. Khennane A, Melchers R. E. A Meso-scale finite element model for environmental stress corrosion of GFRP. *Proceedings of The Fourth Australasian Congress on Applied Mechanics* 2005; 573-578.

[5]. Oh KP. A Monte Carlo study of the strength of unidirectional fiber-reinforced composites. *Journal Composite Mater* 1979; **13:** 311–28.

[6]. Okabe T, Takeda N, Kamoshida Y, Shimizu M, Curtin WA. A 3D shear-lag model considering micro-damage and statistical strength prediction of unidirectional fiber-reinforced composites. *Composite Science Technology* 2001; **61**: 1773–89.

[7]. Okabe T, Takeda N. Size effect on tensile strength of undirectional CFRP composites-experiment and simulation. *Composite Science Technology* 2002; **62**: 2053-64.

[8]. Sekine H, Beaumont P.W.R. A physically based micromechanical theory and diagrams of macroscopic stress-corrosion cracking in aligned continuous glass-fibre-reinforced polymer laminates. *Composite Science and Technology* 1998 ; **58:** 1659-65.

[9]. Swit G. Durability of stresses E-glass fibre in alkaline medium. *In recent Developments in Durability Analysis of Composite Systems. Cardon, Fukuda, Reifsneider and Verchery Editions, Balkema, Rotterdam.* 473-476.

[10]. Weibull W. A statistical distribution of wide applicability. *Journal Applied Mechanics* 1952**; 18:** 293-7.

[11] Wiederhorn S.M, Bolz L.H. Stress corrosion and static fatigue of glass. *Journal of the American Ceramic Society* 1974 ; **57:** 319-323.